Journal of Inflammation Research

Dovepress
Taylor & Francis Group

Open Access Full Text Article

ORIGINAL RESEARCH

Integrative Analysis and Experimental Validation Reveal FCGR1A and ITGAL as Key Inflammatory Biomarkers in Proliferative Diabetic Retinopathy

Han Yu[1,*], Lvyin Luo[2,3,*], Rui Zhang[1,*], Fabao Xu[1], Xueying Yang[1], Yuhan Wu[1], Dechang Han[1], Xuanzhe Chu[1], Jianqiao Li[1]

[1]Department of Ophthalmology, Qilu Hospital, Shandong University, Jinan, People's Republic of China; [2]Department of Neurosurgery, Qilu Hospital, Cheeloo College of Medicine and Institute of Brain and Brain-Inspired Science, Shandong University, Jinan, 250012, People's Republic of China; [3]Shandong Key Laboratory of Brain Function Remodeling, Jinan, People's Republic of China

*These authors contributed equally to this work

Correspondence: Jianqiao Li, Ophthalmology, Qilu Hospital, Shandong University, No. 107, Wenhua West Road, Jinan, Shandong, 250012, People's Republic of China, Email jqli@email.sdu.edu.cn

Purpose: Diabetic retinopathy (DR), one of the most common severe complications of diabetes, has become a leading cause of blindness among the working population without a fundamental treatment. Proliferative DR (PDR) is the advanced stage of DR. Recent studies have shown that inflammation is closely related to PDR, as it promotes leukocyte adhesion, breakdown of the blood-retinal barrier, and pathological neovascularization, but the key regulatory genes involved remained unclear. We aim to identify inflammation-related biomarkers in PDR.

Methods: We downloaded and merged PDR-related datasets GSE102485, GSE94019, and GSE60436, comprising a total of 13 control samples and 37 samples from PDR patients, and conducted a joint analysis of inflammation-related genes (IRGs). Differential analysis, functional enrichment analysis, WGCNA and LASSO were used to identify key genes and their functions in the pathogenesis of PDR. Dataset GSE241239, which contains retinal sequencing data from mice, was used for external validation. Additionally, single-cell RNA analysis using GSE165784, which includes five human-derived PDR samples, was conducted to investigate the cellular expression of Fc Gamma Receptor IA (FCGR1A) and Integrin Subunit Alpha L (ITGAL). Finally, the expression of FCGR1A and ITGAL was validated in DR mouse models and high glucose-induced cell models.

Results: Nine key genes associated with the pathogenesis of PDR were identified. Further screening identified FCGR1A and ITGAL as potential therapeutic targets, with single-cell analysis showing their primary distribution in microglia. In vivo and in vitro experiments confirmed localization of FCGR1A and ITGAL in microglia and significant elevation within DR mouse models.

Conclusion: Comprehensive analysis indicates, for the first time, that FCGR1A and ITGAL are key inflammation-related genes involved in the pathogenesis of PDR mediated by microglia. FCGR1A and ITGAL are promising therapeutic targets for PDR.

Keywords: proliferative diabetic retinopathy, inflammatory, bioinformatics analysis, microglia, DR mouse model

Introduction

Diabetic retinopathy (DR) is a major blinding eye disease and one of the most common complications in diabetic (DM) patients. The development and progression of DR profoundly impact the quality of life for these patients.[1] DR is mainly categorized into two types according to disease progression: non-proliferative DR (NPDR) and proliferative DR (PDR).[2] PDR represents the advanced stage of DR, manifesting neovascularization and vitreous hemorrhage, which further cause retinal detachment and lead to blindness in severe cases.[3] Current treatments mainly incorporate laser therapy and intravitreal administration of anti-vascular endothelial growth factor (VEGF) medications. These treatments are symptomatic treatments, and have obvious flaws, that laser therapy may damage retinal tissue and that anti-VEGF treatment requires frequent injections.[4] Thus, finding new therapeutic targets is of great clinical importance for DR treatment.

Received: 21 February 2025
Accepted: 3 May 2025
Published: 13 May 2025

The pathological features of PDR include neovascularization, fibrovascular membrane formation, and retinal detachment. Previous research has focused primarily on neovascularization. Remarkable, recent studies indicate that infiltration of inflammatory factors promotes PDR progression.[5] Inflammation is a fundamental pathological reaction, representing a defensive response of vascularized tissue to various damaging factors.[6] Under high-glucose conditions, immune cells activate and release substantial quantities of inflammatory mediators and reactive oxygen species, leading to inflammatory responses in retinal tissue.[7] Recent studies suggest that anti-inflammatory therapies are also effective for PDR patients.[8] Notably, the molecular mechanisms underlying the occurrence and progression of PDR remain incompletely understood, and potential anti-inflammatory therapeutic targets in PDR patients merit further investigation.

In this research, we performed an extensive analysis of inflammation's role in PDR by integrating multiple datasets and experimental validations. We uncovered FCGR1A and ITGAL as novel inflammation-related factors in the context of PDR. We also localized these genes using single-cell data, revealing their primary distribution in microglia. Finally, we validated the expression and localization of FCGR1A and ITGAL in diabetic mouse models and microglial cells exposed to high-glucose conditions. This study is the first to reveal the association of FCGR1A and ITGAL, as inflammation-related biomarkers in microglia, with the development of PDR.

Materials and Methods

Data Collection and Processing

The high-throughput sequencing datasets were obtained from the National Center for Biotechnology Information. Datasets GSE102485,[9] GSE60436,[10] GSE94019 [11] contain RNA sequencing data from human PDR and normal tissues (The samples digital information can be found in Supplementary File 1). After performing log2 transformation, removing missing values, and other standardization processes on these datasets, the "inSilicoMerging" R package[12] was used for merging, and batch effects were removed using Combat (based on the empirical Bayes method).[13] GSE241239 [14] is RNA sequencing data oxygen induced retinopathy (OIR) model in C57BL/6 mice, and the single-cell RNA data GSE165784 [15] is derived from the fibrovascular membranes (FVM) of PDR patients. Additionally, by searching "inflammatory" as a keyword on the Gene Ontology Resource, 963 inflammatory-related genes (IRGs) were obtained (The IRGs list can be found in Supplementary File 2)

Differential Expression and Enrichment Analysis

Qualification of DEGs using the "Limma" R package.[16] Using of 1.5-fold differential genes, ie, genes that satisfy the screening criteria [$|\log_2$ (fold change)$| > 0.585$, $p < 0.05$], is considered a cut-off for DEGs. The full list of DEGs and the adjusted p-values can be found in Supplementary File 3. Gene Ontology (GO) and Kyoto Encyclopedia of Genes and Genomes (KEGG) analyses of DEGs were performed using the "clusterProfiler" R package.[17] Pathways with FDR < 0.01 and $p < 0.05$ were deemed statistically significant.

Weighted Gene Co-Expression Network Analysis

Weighted Gene Co-Expression Network Analysis (WGCNA) was applied to analyze gene co-expression across samples, identifying candidate biomarker genes through gene set correlations and phenotype relationships. Outlier genes were removed using the "goodSamplesGenes" function from the "WGCNA" R package,[18] and a scale-free co-expression network was constructed using an optimal soft-threshold power of $\beta = 28$ ($R^2 > 0.85$). Modules highly correlated with PDR were selected as candidate modules; Module Membership (MM) measures the correlation between a gene and a specific module, while Gene Significance (GS) assesses the correlation between a gene and external phenotypes, such as disease status or survival time. Based on empirical criteria that balance selection accuracy and biological significance, thresholds of $|MM| > 0.8$ and $|GS| > 0.20$ were chosen to identify key genes.

LASSO-Cox Regression Analysis

Least Absolute Shrinkage and Selection Operator (LASSO) regression serves as a key technique for selecting relevant variables and applying regularization especially suited for analyzing high-dimensional datasets. R package "glmnet"[19]

was used for LASSO. Key genes with the highest predictive efficiency were ultimately identified based on expression profile data.

Protein-Protein Interaction

The Protein-protein interaction (PPI) network was generated using data from the STRING website,[20] and key genes were identified through the CytoHubba[21] plugin in Cytoscape.[22] As previously described, MCC helps pinpoint nodes exhibiting robust connectivity within the network and participating in numerous densely connected subgraphs. MNC assesses how well the neighbors of a node establish a cohesive component. Degree centrality, as a straightforward indicator, reflects the prominence of a node within the network. EcCentricity serves to distinguish central from peripheral nodes, facilitating insights into the network's architecture and the routes of information flow.[23]

External Dataset Validation

The external validation utilized the GSE241239 dataset. The "pROC" R package[24] was employed to generate ROC curves, with the area under the curve (AUC) calculated to evaluate predictive performance. Candidate genes in differentiating PDR from control samples. An AUC above 0.7 was considered to reflect acceptable predictive accuracy.

Gene Set Enrichment Analysis (GSEA)

GSEA was conducted to explore the potential functional roles of diagnostic genes,[25] utilizing reference gene sets sourced from the Molecular Signatures Database (MSigDB).[26] For single-gene GSEA (sg-GSEA), samples were divided into high expression ($\geq$ 50%) and low expression ($<$ 50%) groups based on their gene expression levels. This analysis aimed to investigate the pathways and molecular mechanisms related to these genes. |NES| (Normalized Enrichment Score) $>$ 1 was considered significant, while $p < 0.05$ was statistically significant.

Transcription Factors (TFs) and Drug Network

The TFs were predicted using miRNet. Small-molecule drugs were searched using the gene names in the DGIdb.

Single-Cell Analysis

GSE165784 acquisition of single-cell RNA data using the R package "Seurat" (version 5.2.0).[27] Cells of low quality were filtered based on the criteria (200 $<$ nFeature RNA $<$ 6000, nCount_RNA $<$ 50,000, and percent.mt $<$ 30), followed by normalization using the "SCTransform" method and subsequent logarithmic transformation. Cell clusters were determined using the "FindClusters" function with a resolution of 0.5. Unsupervised clustering was employed to display cell markers within each cluster, and then cell types were mapped into individual cell clusters, manually annotated, and HUB genes mapped in a single-cell landscape.

Establishment of a Streptozotocin (STZ) Induced DR Mouse Model

This study was approved by the Animal Ethics Committee of Qilu Hospital, Shandong University. We adhered to the "3R" principles to reduce animal suffering. Six-week-old C57BL/6J mice were fed a high-fat diet (HFD) consisting of 60 kcal% fat for 4 weeks. Starting from the fifth week, the mice received daily intraperitoneal injections of low-dose STZ (40 mg/kg) for 4 consecutive days. The STZ was dissolved in a 0.05 mol/L citrate buffer (pH 4).[28]

Cell Culture

Primary microglial cells were isolated from 1–3 day-old neonatal mice. Whole brain tissue was placed in Hank's Balanced Salt Solution, and gray matter was separated, digested with trypsin, and triturated to remove large fragments. After digestion, cortical cells were filtered, centrifuged, and resuspended to obtain a single-cell suspension, then seeded into culture flasks. Following 24 hours of adhesion, granulocyte-macrophage colony-stimulating factor (GM-CSF) was added, and cells were cultured for 7–8 days. According to the previously mentioned high-glucose-induced cell culture protocol.[29] Microglia were collected after shaking for 2–3 hours, centrifuged, and split into two groups: one in high-

glucose (30 mm) medium and one in regular medium. After 48 hours, immunofluorescence staining and Western blotting were performed.

Immunofluorescence (IF)

Cells or tissue sections were fixed in 4% paraformaldehyde, permeabilized using 0.5% Triton X-100, blocked with donkey serum, and subsequently incubated with primary antibodies overnight at 4°C. Using these primary antibodies: mouse anti-ITGAL (1:50, Santa Cruz, US), mouse anti-FCGR1A (1:100, Thermo Fisher, US), rabbit anti-FCGR1A (1:100, Abclonal, China), and rabbit anti-Iba1 (1:500, Wako, Japan). Sections were then treated with the respective secondary antibodies: goat anti-mouse IgG labeled with 594 (1:100, Abclonal, China) and goat anti-rabbit IgG labeled with Alexa Fluor 488 (1:300, Abclonal, China). Imaging was conducted using a fluorescence microscope.

Western Blot

Proteins were extracted from cells or tissues with RIPA lysis buffer, combined with loading buffer, and heated at 95°C for 10 minutes to denature. Samples were subjected to gel electrophoresis, transferred to a PVDF membrane, blocked with BSA for 1 hour at room temperature, and incubated overnight at 4°C with primary antibodies (rabbit anti-ITGAL and anti-FCGR1A, 1:1000, Abclonal, China). After washing with TBS-Tween 20, membranes were treated with secondary antibodies for 2 hours. Membranes were then visualized using ECL substrate (Abbkine, China) and the ChemiDocTM MP Imaging System (Bio-Rad, USA).

HE Staining

The eyeballs were collected from the animals and fixed in 4% paraformaldehyde, then embedded in paraffin for sectioning. Paraffin sections were baked on a 60°C slide warmer, deparaffinized in xylene and gradually rehydrated through a series of ethanol concentrations (100%, 95%, 80%, and 70%). Next, these sections were immersed into hematoxylin solution for 10 minutes for nuclear staining, rinsed in running water, briefly differentiated in 1% hydrochloric acid ethanol, rinsed again, and blued.

Statistical Analysis

Statistical analyses were conducted using GraphPad Prism 9.0 and R software (version 4.4.1) with default parameters, unless specified. Data analysis and visualization were also supported by SangerBox website.[30] All data are presented as Mean ± Standard Error of the Mean (SEM), and statistical significance was determined using unpaired two-tailed Student's *t*-test or one-way ANOVA test, and $p < 0.05$ was considered significant.

Results

Datasets Integration and Batch Effect Removal

We merged datasets GSE102485, GSE94019, and GSE60436, removing batch effects. Initially, box and density plots showed significant distribution differences, which became consistent post-adjustment, with aligned medians and uniform density across samples (Figure 1A and B). The combined dataset included 37 PDR samples and 13 normal retinal controls.

Differential and Enrichment Analysis of IRGs in PDR

Analysis identified 2153 upregulated and 462 downregulated DEGs (Figure 2A and B). By intersecting these DEGs with IRGs, we identified 222 differentially expressed inflammation-related genes (DEIRGs) (Figure 2C). KEGG analysis showed that DEIRGs were enriched in pathways like Tuberculosis, NOD-like receptor signaling, and Toxoplasmosis (Figure 2D). GO analysis of DEIRGs revealed enrichment in biological processes such as inflammatory response, defense response, and response to stress (Figure 2E). Enrichment results are available in Supplementary File 4.

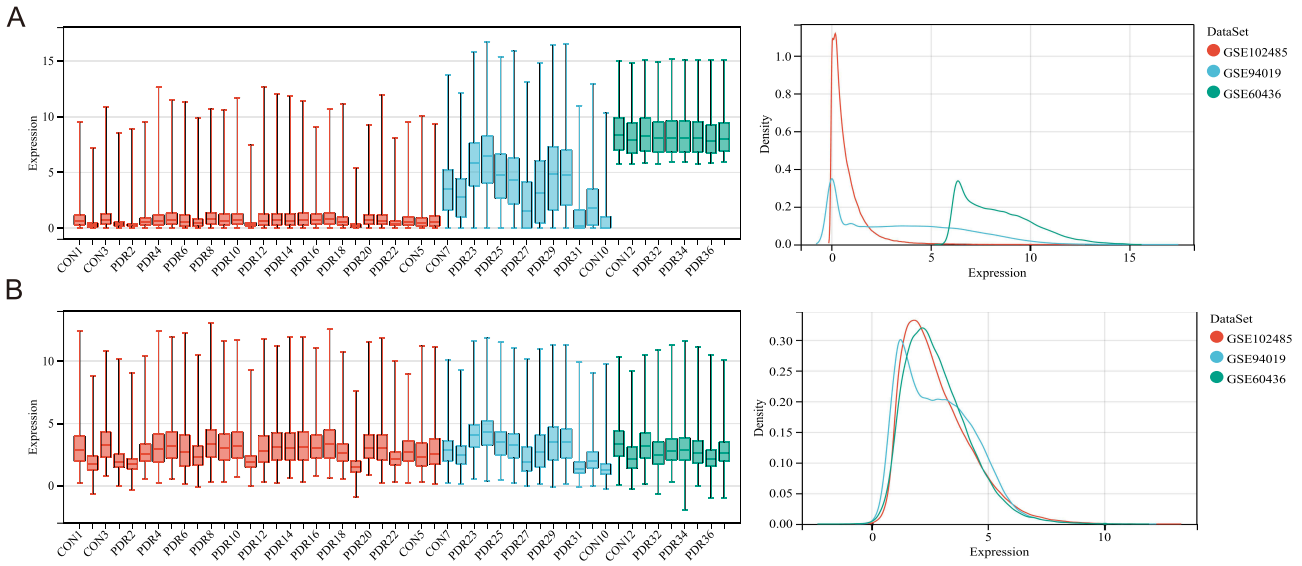

Figure 1 Identification and Enrichment Analysis of IRGs. (**A**) Bar plots and density plots of three datasets before batch correction. (**B**) Bar plots and density plots of the merged dataset after batch correction.

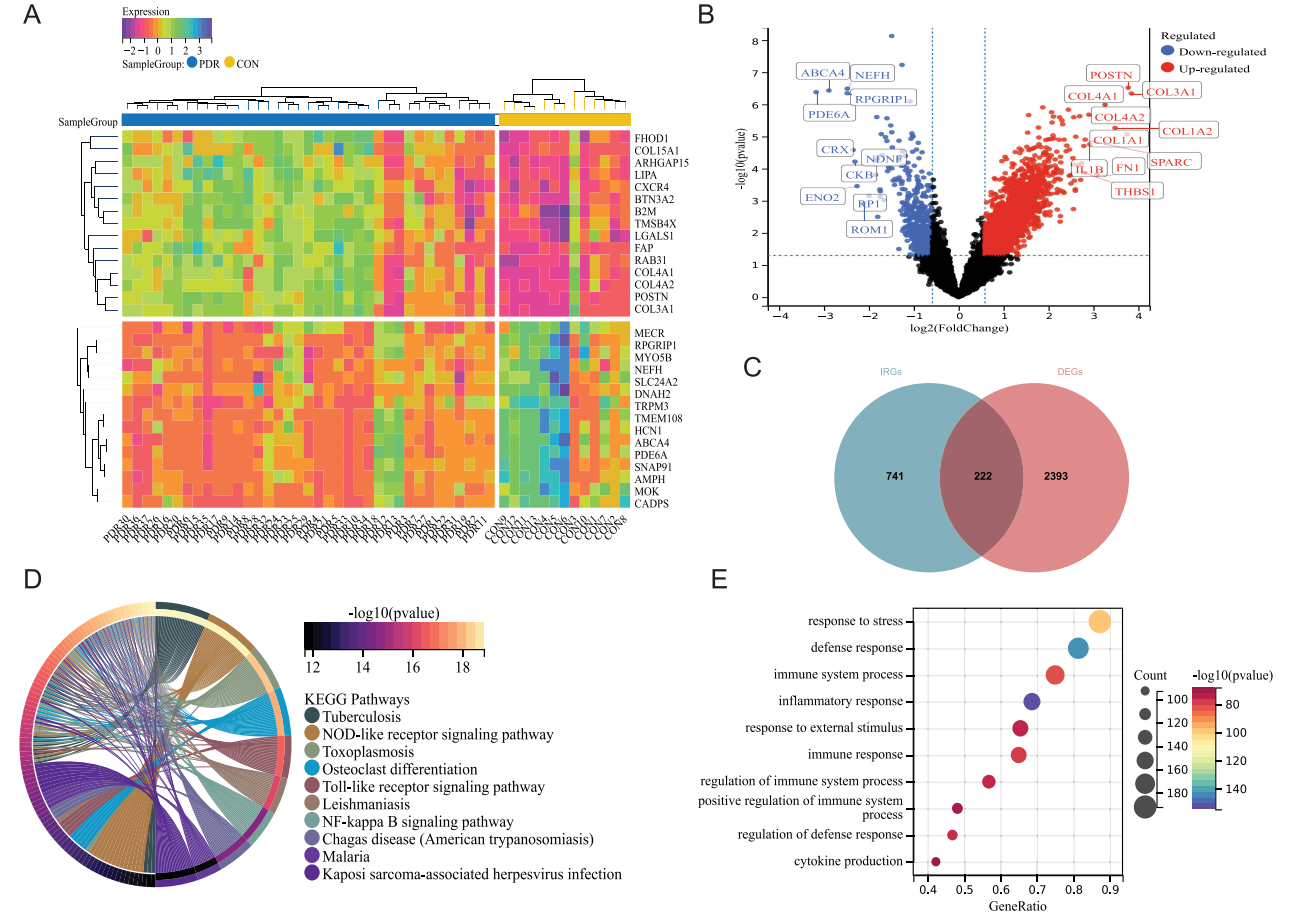

Figure 2 Identification and Enrichment Analysis of IRGs. (**A**) Heatmap showing the top 15 upregulated and downregulated differential genes. (**B**) Volcano plot of differential genes. (**C**) Venn diagram showing the upregulated and downregulated IRGs. (**D**) Chord diagram of KEGG enrichment analysis. (**E**) GO analysis of different expression IRGs.

https://doi.org/10.2147/JIR.S519725

WGCNA Analysis

WGCNA constructs gene co-expression networks to identify modules that exhibit strong associations with specific phenotypes, and selects key genes with potential biological significance. The scale-free network was optimized at a soft threshold power of β = 28 (Figure 3A), identifying 13 modules from 50 samples (Figure 3B). Modules were associated with external traits to identify biomarkers, with "PDR" as a trait showing the strongest correlations in the dark red (Cor = 0.5, P = 2.4e − 4) and green modules (Cor = 0.49, P = 3.3e − 4) (Figure 3C–E). We extracted hub genes from these modules (GS > 0.20, MM > 0.80), totaling 525 genes (Supplementary File 5). Nine key genes—AIF1, CD2AP, ELF4, FCGR1A, ITGAL, LY86, NLRP3, OSMR, and PLEKHO2—were identified by intersecting hub genes with IRDEGs (Figure 3F).

Key Gene Selection Through LASSO and PPI

Pearson correlation analysis indicated correlations among the 9 hub genes (Figure 4A). LASSO-Cox analysis, using an optimal lambda of 0.05, identified 4 genes——ELF4, FCGR1A, ITGAL, and NLRP3 (Figure 4B and C; LASSO scores in Supplementary File 6). The 9 IRDEGs were input into the STRING website to construct a PPI network. Using the MCC algorithm in CytoHubba, the top five interacting proteins were ITGAL, FCGR1A, AIF1, NLRP3, and LY86 (Figure 4D), confirmed by MNC, degree, and eccentricity algorithms (Supplementary File 7). Ultimately, three key genes —ITGAL, FCGR1A, and NLRP3—were highlighted (Figure 4E). Validation in internal and external datasets showed good diagnostic performance for ITGAL (0.81), FCGR1A (0.79), and NLRP3 (0.80) in the merged dataset. In GSE241329 (OIR mice), ITGAL and FCGR1A demonstrated AUCs of 0.89 and 1.00, respectively, while NLRP3 showed an AUC of 0.64, supporting ITGAL and FCGR1A as potential PDR biomarkers, though further validation is required (Figure 4F). Finally we compared the expression levels of these three genes in a human merged dataset and a mouse model dataset. The results showed that the overall expression levels of these key genes were higher in human tissues, while NLRP3 did not exhibit significant changes in the mouse model (Figure 4G and H).

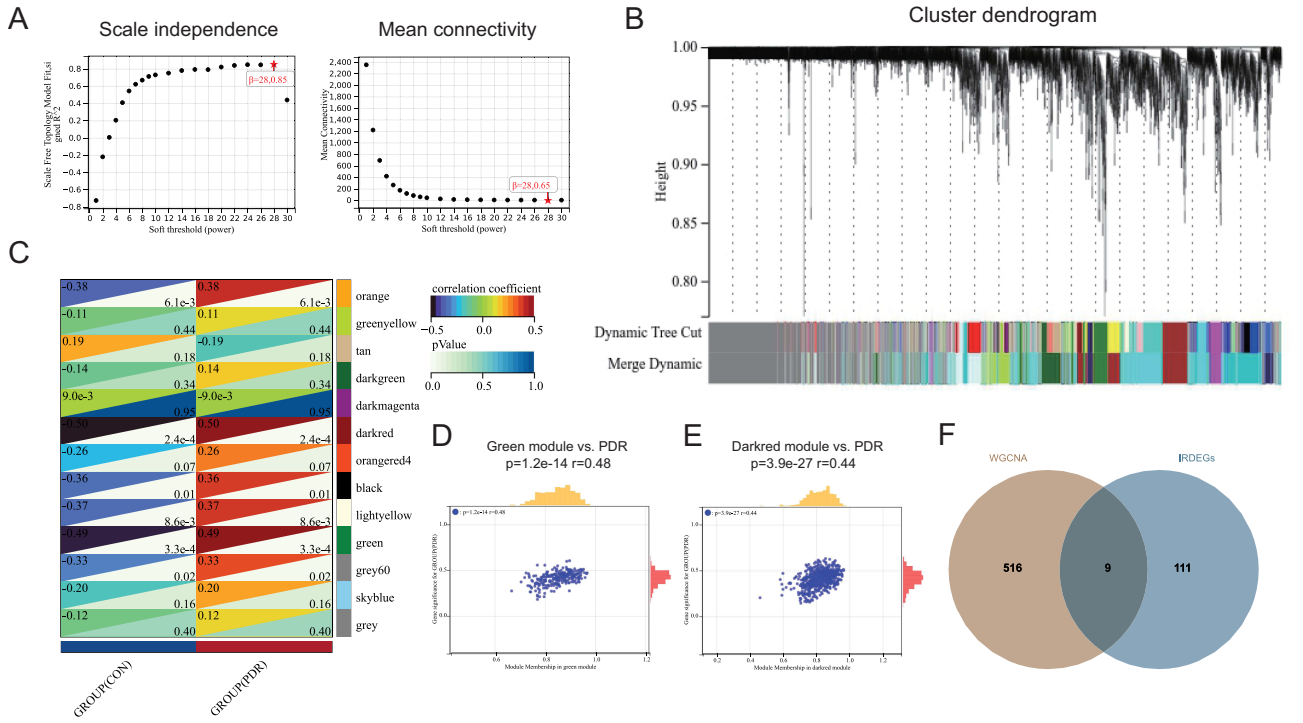

Figure 3 WGCNA analyses of merge datasets. (**A**) Selection of the optimal soft threshold power (β). (**B**) Clustering tree displaying the identified 13 modules. (**C**) Pearson correlation analysis of modules with clinical characteristics. (**D**) Correlation of the green module with PDR. (**E**) Correlation of the darkred module with PDR. (**F**) Further screening of 9 hub genes.

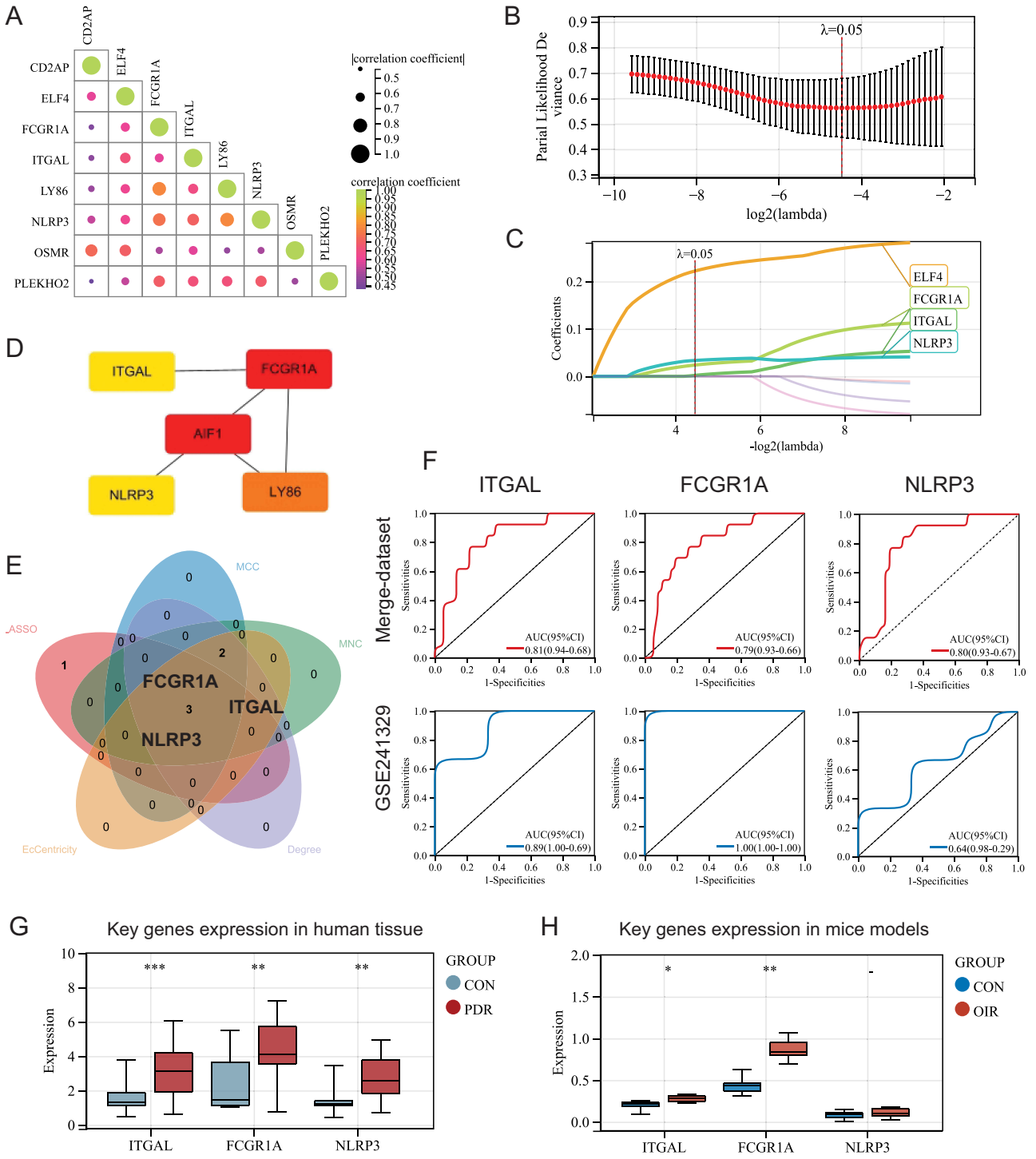

Figure 4 Selection of Key Genes through LASSO and PPI. (**A**) Correlation of the 9 genes. (**B**) LASSO analysis determined the soft threshold capability (lambda = 0.05). (**C**) According to soft threshold capability (lambda = 0.05) identified 4 key genes. (**D**) MCC algorithm of PPI network selected top 5 genes. (**E**) Venn diagram illustrating the intersection of LASSO with various PPI algorithms. (**F**) ROC curves of ITGAL and FCGR1A in the merged dataset and external validation dataset (GSE241329). AUC > 0.7 is considered indicative of good predictive performance. (**G**) ITGAL, FCGR1A and NLRP3 expression in the human merged dataset (**H**) ITGAL, FCGR1A and NLRP3 expression in the mouse model dataset *p < 0.05, **p < 0.01, ***p < 0.001.

Functional Identification of Hub Genes: Sg-GSEA and Small Molecule Drug Prediction

We conducted sg-GSEA analysis on ITGAL (Integrin Subunit Alpha L) and FCGR1A (Fc Gamma Receptor IA) to investigate their roles in PDR. Samples were divided into high (≥ 50%) and low (< 50%) expression groups based on gene expression. In the high-expression group of FCGR1A, the top three enriched pathways were ALLOGRAFT

https://doi.org/10.2147/JIR.S519725

REJECTION (|NES|=1.8793, p=0.0042), INFLAMMATORY RESPONSE (|NES|=1.9396, p<0.001), and INTERFERON RESPONSE (|NES|=1.9485, p=0.0081) (Figure 5A). For ITGAL, the enriched pathways included COMPLEMENT (|NES|=2.0399, p<0.001), INFLAMMATORY RESPONSE (|NES|=2.0386, p<0.001), and INTERFERON RESPONSE (|NES|=2.152, p<0.001) (Figure 5B). Detailed GSEA results are in Supplementary File 8. Additionally, we constructed a TF-small molecule drug network, where RFX1 targets ITGAL and SPI1 and STAT1 target FCGR1A. The top-interacting molecule with FCGR1A was MDX-447 (score = 15.75), and with ITGAL was CASEARINOL B (score = 3.62) (Figure 5C). Full TF and drug interaction data are in Supplementary File 9.

Single-Cell Data Reveal the Key Role of FCGR1A and ITGAL are Expressed in Microglia

GSE165784 is a single-cell sequencing dataset from the 5 vitreous FVMs of PDR patients. Low-quality cells were screened out using the criteria as mentioned above (Figure 6A). Next, the SCTransform standardization of the data and the PCA and umap dimensionality reduction processing are carried out. It was divided into 15 clusters through unsupervised clustering (Figure 6B). Based on the original study by Hu et al,[15] we performed manual annotation of cells (Figure 6C and D) and identified a total of 7 cell populations, including microglia (C1QA, TREM2, GPR34), monocyte/macrophage (LYZ, FCN1, VCAN), fibroblast (COL1A1, COL1A2, FN1), pericyte (FCER1A, NAPSB, CD1C), endothelium (VWF, CLDN5, SPARCL1), DC (RGS5, CALD1, THY1), and T&NK cells (TRBC2, LTB, CD2) (Figure 6E). Mapping FCGR1A and ITGAL to the single-cell landscape revealed that they were predominantly distributed in the microglia cluster (Figure 6F). The dot plot further demonstrated that FCGR1A and ITGAL were more highly expressed in immune cells compared to other cell types, including microglia, M0/macrophages, and T/NK cells. Notably, FCGR1A showed significantly higher expression in microglia (Figure 6G).

Successfully Established a DR Mouse Model

To validate the expression of FCGR1A and ITGAL in DR animals, we used STZ-induced diabetic mice for 16 weeks, monitoring blood glucose levels weekly, the fasting blood glucose levels of the diabetic group mice were all ≥ 13.9 mmol/L (Figure 7A). Histological examination via HE staining showed that the thickness of the inner nuclear layer, outer nuclear layer, and neural retina in diabetic mice was reduced compared to normal mice, confirming the successful modeling of DR (n=3, p<0.01 Figure 7B–E).

In vivo Model Validation Showed That FCGR1A and ITGAL are Highly Expressed in the Retina of DR

We performed IF on mouse retinal tissue sections. IF analysis revealed increased expression of FCGR1A and ITGAL in the inner nuclear layer of DR mice (Figure 8A). We extracted mouse retinal proteins for WB analysis, and the WB results demonstrated increased expression of ITGAL and FCGR1A in DR mice (n=6, p<0.001, Figure 8B–D).

The in vitro Model Showed That FCGR1A and ITGAL are Expressed in Microglia, with Elevated Expression Levels in the High-Glucose Treatment Group

To correlate with the previous single-cell results, we extracted primary microglia, treated with high-glucose (HG) DMEM (30 mmol/L glucose) for 48 hours, and immunofluorescence validation showed co-localization of Iba1 with ITGAL and FCGR1A, indicating their expression in microglia (Figure 9A). In vitro, the control group was treated with standard medium (5.5mmol/L glucose), while the high-glucose group was treated with HG DMEM (30 mmol/L glucose) for 48 hours. After 48 hours, proteins were isolated for Western blot (WB) analysis, revealing a marked elevation in ITGAL and FCGR1A protein levels in the HG group. (n=3, p<0.001, Figure 9B–D).

Discussion

The pathogenesis of PDR is complicated, and recent evidence suggests that inflammation is a key factor contributing to PDR. A hyperglycemic environment leads to the activation of immune cells, releasing a large amount of inflammatory

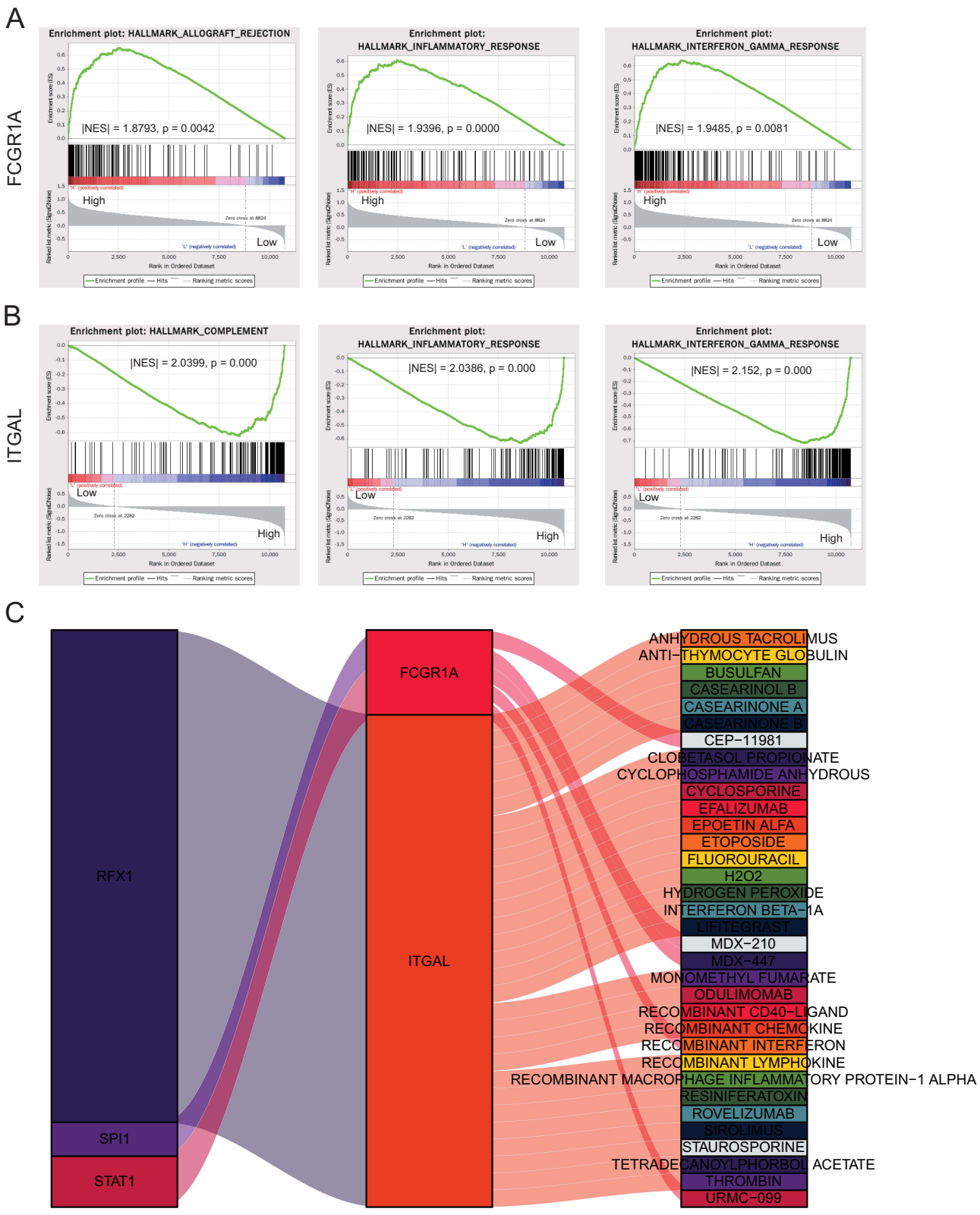

Figure 5 Functional Identification of Hub Genes. (**A**) sg-GSEA of FCGR1A. (**B**) sg-GSEA of ITGAL. (**C**) Sankey diagram illustrating the prediction of TF and small molecules.

mediators and resulting in an inflammatory response in retinal tissue.[31] Microglia, as resident immune cells in the retina, participates in the occurrence and progenesis of retinal inflammation.[32,33] However, the gene regulating microglia-mediated inflammation remained unclear.

https://doi.org/10.2147/JIR.S519725

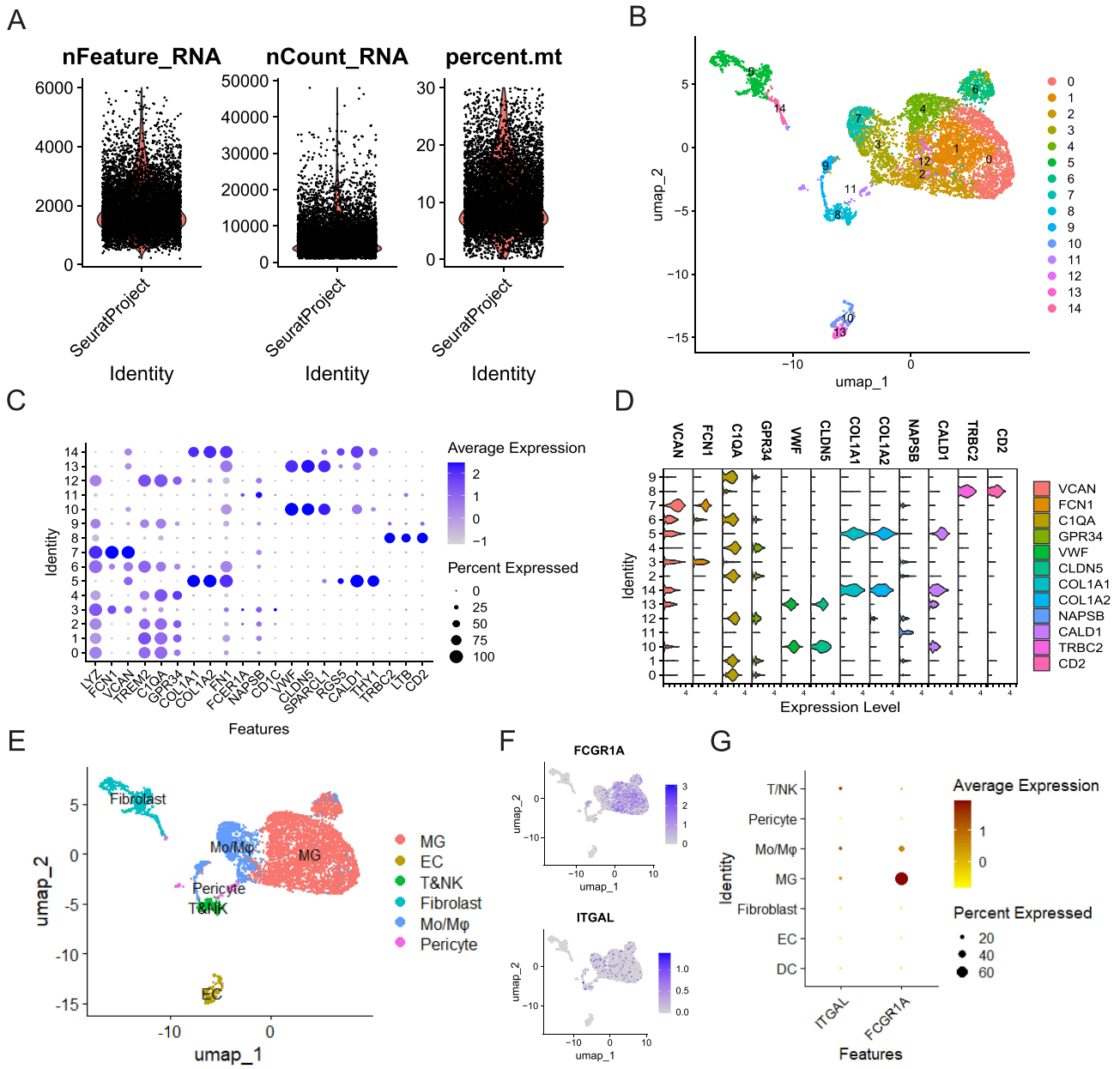

Figure 6 Single-Cell Analyses. (**A**) Single-cell data after screening out low-quality cells. (**B**) Fifteen cell clusters were identified by unsupervised clustering. (**C**) Dot plot shows cell annotation markers. (**D**) VInplot shows cell annotation markers. (**E**) Landscape of 7 cell types in umap. (**F**) Localization of FCGR1A and ITGAL in cells. (**G**) Dot plot demonstrating the expression levels of FCGR1A and ITGAL across various cell types.

In this study, we merged datasets GSE102485, GSE94019, and GSE60436 to identify DEGs enriched in pathways related to inflammatory and defense responses. Our findings further confirm that PDR is an inflammatory lesion, aligning with previous studies.[34,35] We identified FCGR1A and ITGAL as potential biomarkers for PDR through methods such as WGCNA, PPI, and LASSO. Furthermore, DR mouse model and hyperglycemia-induced primary microglia confirm that elevated levels of FCGR1A and ITGAL are linked to PDR pathogenesis. Under hyperglycemic conditions, the expression of these genes increased both in vivo and in vitro.

The FCGR1A gene encodes a high-affinity Fc-γ receptor that is predominantly expressed on immune cells, including macrophages, monocytes, and dendritic cells. It mediates antibody-dependent cellular phagocytosis and cytotoxic responses by binding to immunoglobulin G (IgG).[36] During the inflammatory response, FCGR1A can recognize and bind to pathogen surface antigen-antibody complexes, activating immune cells and promoting the release of

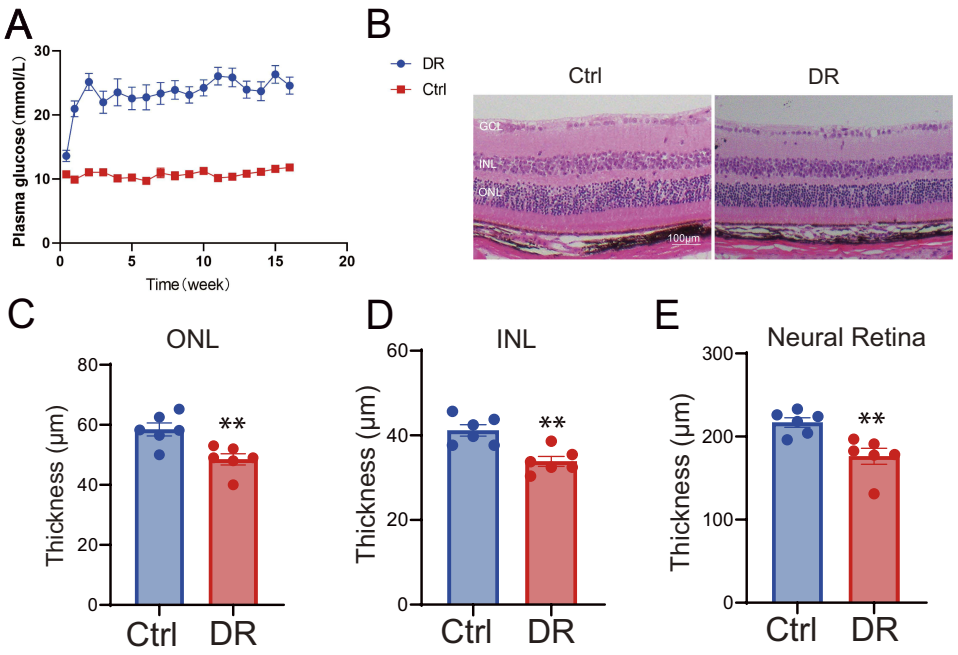

Figure 7 DR model. (**A**) Blood glucose levels of control and DR mice each week after STZ injection. (**B**–**E**) HE staining of paraffin section of the retina of control and DR mice. Quantification of the thickness of the outer nuclear layer (ONL), inner nuclear layer (INL) and the neural retina. **P< 0.001. Data are shown as mean ± SEM.

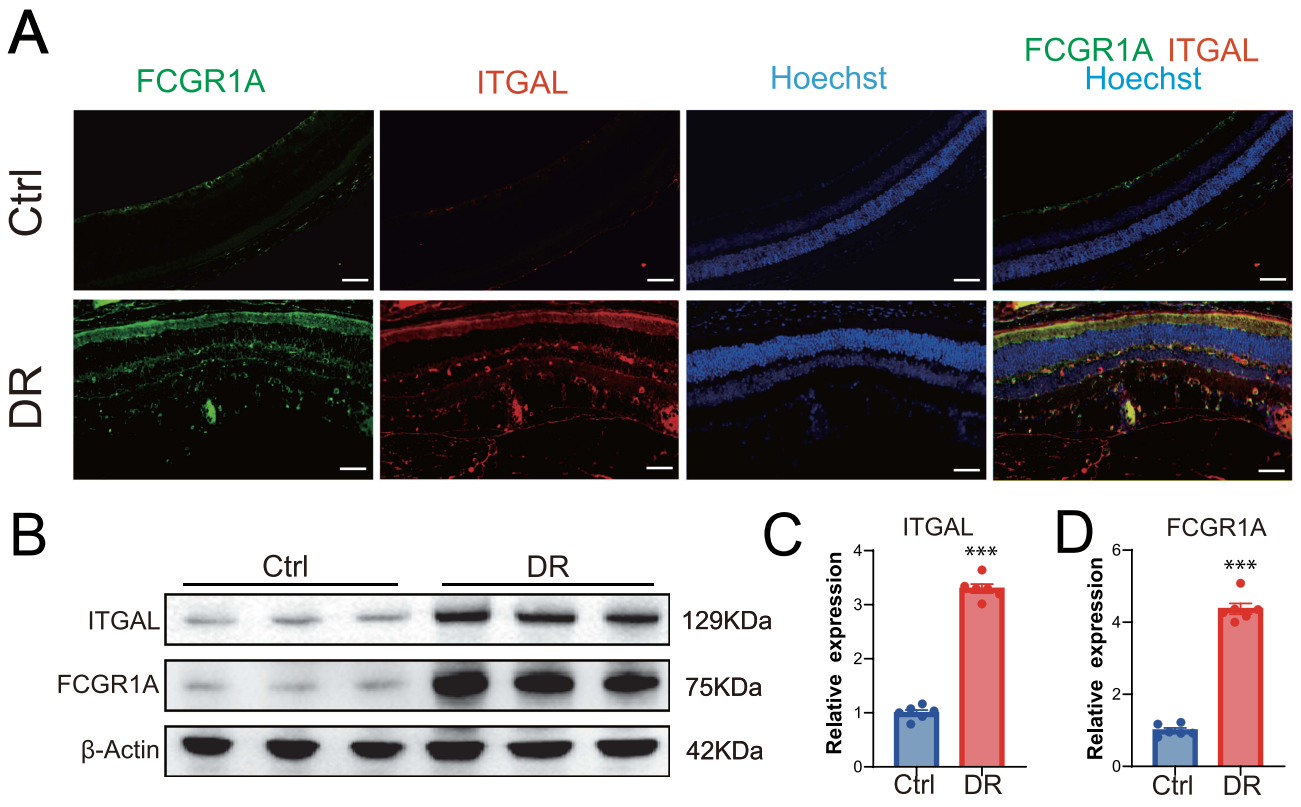

Figure 8 The expression of FCGR1A and ITGAL in mouse retina. (**A**) Immunofluorescence validation of ITGAL and FCGR1A expression in the paraffin section of mouse retina (scale bar: 100μm). (**B**) Western blots verified the protein expression levels of ITGAL and FCGR1A in different groups of mice. (**C** and **D**) Quantification of the expression of ITGAL and FCGR1A, n=6/group. Statistical significance was evaluated by paired *t*-test. ***P< 0.001. Data are shown as mean ± SEM.

https://doi.org/10.2147/JIR.S519725

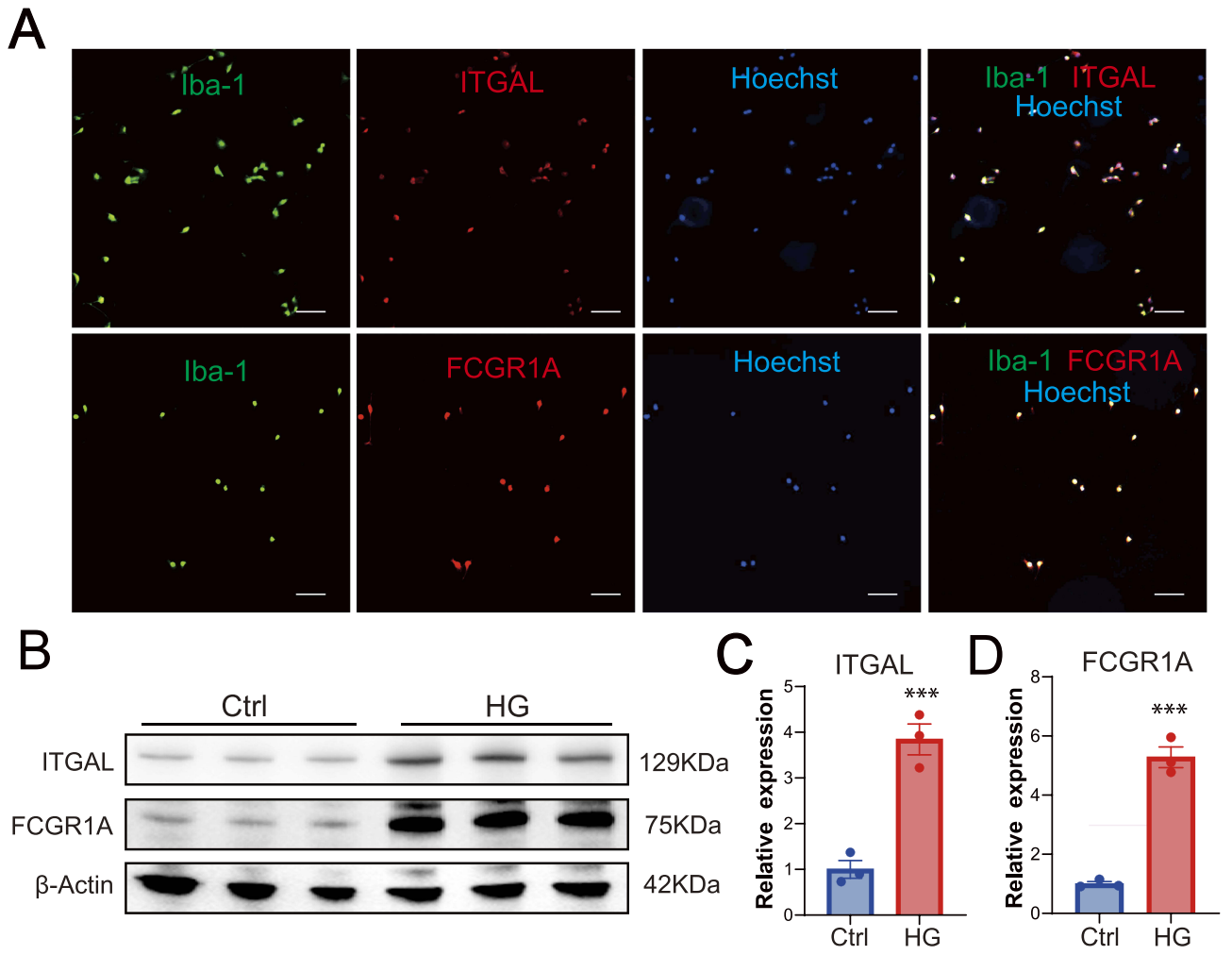

Figure 9 The expression of FCGR1A and ITGAL in HG treated microglia (**A**) Co-localization of ITGAL and FCGR1A with Iba1 in primary microglia (scale bar: 100μm). (**B**) Western blots of microglia treated with normal glucose and HG. (**C** and **D**) Quantification of the expression of ITGAL and FCGR1A, n=3/group. Statistical significance was evaluated by paired *t*-test. ***P< 0.001. Data are shown as mean ± SEM.

inflammatory factors to enhance the immune response.[37] Additionally, FCGR1A is significantly involved in chronic inflammation and autoimmune disorders, including rheumatoid arthritis and systemic lupus erythematous (SLE).[38,39] So far, the downstream mechanism remains unclear. The ITGAL gene encodes the integrin alpha L subunit (commonly referred to as CD11a), which forms a lymphocyte function-associated antigen-1 (LFA-1) complex with CD18. During inflammation, LFA-1 enhances the migration and infiltration of immune cells to the site of inflammation by binding to intercellular adhesion molecule-1 (ICAM-1), thereby strengthening cell-cell interactions.[40] In certain autoimmune diseases like SLE, high expression of ITGAL is associated with abnormal immune responses.[41] Downstream mechanisms still need to be further explored.

We conducted further targeted small-molecule drug predictions and identified MDX-447 and Casearinol B as potential therapeutic agents. MDX-447 is a bispecific antibody originally designed to target FCGR1A and EGFR, and has been studied in the context of hematologic malignancies.[42] Although its role in retinal diseases has not been explored, our drug-gene interaction prediction suggested a strong potential binding affinity (score = 15.75) to FCGR1A, indicating its possible repurposing value in inflammatory contexts such as PDR. CASEARINOL B is a natural compound with reported anti-inflammatory properties.[43] It was predicted to interact with ITGAL (score = 3.62), a gene involved in leukocyte adhesion and immune activation. While experimental validation is still required, its potential to modulate ITGAL-related pathways may provide therapeutic implications in microglia-driven retinal inflammation. In our study, we

also screened NLRP3, a known inflammatory regulator, and found that it may play a regulatory role in PDR, and further studies are needed to determine its potential as a PDR target.

Further single-cell analysis shows that both FCGR1A and ITGAL are distributed in microglia, with FCGR1A exhibiting very high expression levels in microglia. The expression level of ITGAL in microglia is not as high as that of FCGR1A, primarily because the overall expression of ITGAL in the retina is relatively low. However, this does not rule out the possibility that ITGAL plays a crucial role in the progression of PDR. To investigate this, we extracted retinas from DR mice and microglial cells for further validation. The results showed that ITGAL expression was elevated in PDR and localized to microglia. Microglia develops from mesenchymal stem cells of the mesoderm and migrates into the central nervous system, where they adapt to the CNS environment and function as macrophages.[44,45] In recent years, the role of microglia in PDR has gradually been revealed. A high-glucose environment activates microglial cells, which release TNF-α, IL-1β, and inducible nitric oxide synthase (iNOS), damaging retinal pericytes and vascular endothelial cells. This promotes endothelial damage and increased permeability, resulting in fragile, leaky vessel walls, exacerbating retinal inflammation, and advancing disease progression.[46] Importantly, various retinal cell types, including endothelial cells, astrocytes, and neurons, can react to the initial activation of microglia by contributing to and intensifying the inflammatory response. In addition, microglia has been shown to possess both pro-fibrotic and fibrogenic characteristics that contribute to the formation of FVM.[15] Targeting molecules that regulate microglial activation or associated pro-inflammatory factors may provide insights for the development of targeted therapies for microglia in PDR.[32]

In summary, we found that FCGR1A and ITGAL are highly expressed in the DR retina and microglia treated with high glucose, and the consistent upregulation of FCGR1A and ITGAL across multiple datasets and their strong diagnostic performance suggest that these genes may serve as promising diagnostic biomarkers for PDR. Furthermore, given their involvement in microglial activation and inflammatory pathways, they also hold potential as therapeutic targets for modulating retinal inflammation in PDR. Our study offers new insights into PDR pathogenesis research and targeted drug design. However, this study has several limitations. First, the mechanisms by which FCGR1A and ITGAL regulate inflammation in PDR were not explored in depth, their effects on microglial cytokine secretion warranting further investigation in the future. Second, due to the cross-sectional design of the integrated datasets, causal relationships between the identified biomarkers and PDR progression cannot be firmly established. Future longitudinal studies are needed to validate these findings and explore their temporal dynamics.

Ethics Approval

This study was approved by the Animal Ethics Committee of Qilu Hospital, Shandong University, under ethical approval number (DWLL-2024-084). This study also utilized publicly available datasets from the GEO database, and no private or identifiable information was involved. According to the Measures for Ethical Review of Life Science and Medical Research Involving Human Subjects (Article 32, Items 1 and 2), this study is exempt from ethical approval.

Acknowledgments

This study was supported by grants from Young Scientists Fund of National Natural Science Foundation of China (Grant No. 82201169), National Natural Science Foundation of China (Grant No. 82471090), the Fellowship of China Postdoctoral Science Foundation (Grant No. 2022M711952), the Fellowship of China Postdoctoral Science Foundation (Grant No. 2022TQ0198), Natural Science Foundation of Shandong Province (Grant NO. ZR2024QH580).

Disclosure

The authors report no conflicts of interest in this work.

References

1. Cheung N, Mitchell P, Wong TY. Diabetic retinopathy. *Lancet*. 2010;376(9735):124–136. doi:10.1016/S0140-6736(09)62124-3
2. Vujosevic S, Aldington SJ, Silva P, et al. Screening for diabetic retinopathy: new perspectives and challenges. *Lancet Diabetes Endocrinol*. 2020;8(4):337–347. doi:10.1016/S2213-8587(19)30411-5

3. Sharma I, Yadav KS, Mugale MN. Redoxisome and diabetic retinopathy: pathophysiology and therapeutic interventions. *Pharmacol Res*. 2022;182:106292. doi:10.1016/j.phrs.2022.106292
4. Nawaz IM, Rezzola S, Cancarini A, et al. Human vitreous in proliferative diabetic retinopathy: characterization and translational implications. *Prog Retin Eye Res*. 2019;72:100756. doi:10.1016/j.preteyeres.2019.03.002
5. Vujosevic S, Simó R. Local and systemic inflammatory biomarkers of diabetic retinopathy: an integrative approach. *Invest Ophthalmol Vis Sci*. 2017;58(6):Bio68–bio75. doi:10.1167/iovs.17-21769
6. Xiong P, Zhang F, Liu F, et al. Metaflammation in glucolipid metabolic disorders: pathogenesis and treatment. *Biomed Pharmacother*. 2023;161:114545. doi:10.1016/j.biopha.2023.114545
7. Chen M, Luo C, Zhao J, et al. Immune regulation in the aging retina. *Prog Retin Eye Res*. 2019;69:159–172. doi:10.1016/j.preteyeres.2018.10.003
8. Yue T, Shi Y, Luo S, et al. The role of inflammation in immune system of diabetic retinopathy: molecular mechanisms, pathogenetic role and therapeutic implications. *Front Immunol*. 2022;13:1055087. doi:10.3389/fimmu.2022.1055087
9. Li Y, Chen D, Sun L, et al. Induced expression of VEGFC, ANGPT, and EFNB2 and their receptors characterizes neovascularization in proliferative diabetic retinopathy. *Invest Ophthalmol Vis Sci*. 2019;60(13):4084–4096. doi:10.1167/iovs.19-26767
10. Ishikawa K, Yoshida S, Kobayashi Y, et al. Microarray analysis of gene expression in fibrovascular membranes excised from patients with proliferative diabetic retinopathy. *Invest Ophthalmol Vis Sci*. 2015;56(2):932–946. doi:10.1167/iovs.14-15589
11. Lam JD, Oh DJ, Wong LL, et al. Identification of RUNX1 as a mediator of aberrant retinal angiogenesis. *Diabetes*. 2017;66(7):1950–1956. doi:10.2337/db16-1035
12. Taminau J, Meganck S, Lazar C, et al. Unlocking the potential of publicly available microarray data using inSilicoDb and inSilicoMerging R/Bioconductor packages. *BMC Bioinf*. 2012;13(1):335. doi:10.1186/1471-2105-13-335
13. Johnson WE, Li C, Rabinovic A. Adjusting batch effects in microarray expression data using empirical Bayes methods. *Biostatistics*. 2007;8(1):118–127. doi:10.1093/biostatistics/kxj037
14. Zhu W, Gui X, Zhou Y, et al. Aurora kinase B disruption suppresses pathological retinal angiogenesis by affecting cell cycle progression. *Exp Eye Res*. 2024;239:109753. doi:10.1016/j.exer.2023.109753
15. Hu Z, Mao X, Chen M, et al. Single-cell transcriptomics reveals novel role of microglia in fibrovascular membrane of proliferative diabetic retinopathy. *Diabetes*. 2022;71(4):762–773. doi:10.2337/db21-0551
16. Ritchie ME, Phipson B, Wu D, et al. limma powers differential expression analyses for RNA-sequencing and microarray studies. *Nucleic Acids Res*. 2015;43(7):e47. doi:10.1093/nar/gkv007
17. Yu G, Wang L-G, Han Y, et al. clusterProfiler: an R package for comparing biological themes among gene clusters. *Omics*. 2012;16(5):284–287. doi:10.1089/omi.2011.0118
18. Langfelder P, Horvath S. WGCNA: an R package for weighted correlation network analysis. *BMC Bioinf*. 2008;9(1):559. doi:10.1186/1471-2105-9-559
19. Tibshirani R. The lasso method for variable selection in the cox model. *Stat Med*. 1997;16(4):385–395. doi:10.1002/(SICI)1097-0258(19970228)16:4<385::AID-SIM380>3.0.CO;2-3
20. Szklarczyk D, Franceschini A, Wyder S, et al. STRING v10: protein–protein interaction networks, integrated over the tree of life. *Nucleic Acids Res*. 2014;43(D1):D447–D452. doi:10.1093/nar/gku1003
21. Chin CH, Chen S-H, Wu -H-H, et al. cytoHubba: identifying hub objects and sub-networks from complex interactome. *BMC Syst Biol*. 2014;4(Suppl 4):S11. doi:10.1186/1752-0509-8-S4-S11
22. Shannon P, Markiel A, Ozier O, et al. Cytoscape: a software environment for integrated models of biomolecular interaction networks. *Genome Res*. 2003;13(11):2498–2504. doi:10.1101/gr.1239303
23. Luo L, Ma X, Kong D, et al. Multiomics integrated analysis and experimental validation identify TLR4 and ALOX5 as oxidative stress-related biomarkers in intracranial aneurysms. *J Neuroinflammation*. 2024;21(1):225. doi:10.1186/s12974-024-03226-0
24. Robin X, Turck N, Hainard A, et al. pROC: an open-source package for R and S+ to analyze and compare ROC curves. *BMC Bioinf*. 2011;12(1):77. doi:10.1186/1471-2105-12-77
25. Subramanian A, Tamayo P, Mootha VK, et al. Gene set enrichment analysis: a knowledge-based approach for interpreting genome-wide expression profiles. *Proc Natl Acad Sci U S A*. 2005;102(43):15545–15550. doi:10.1073/pnas.0506580102
26. Liberzon A, Birger C, Thorvaldsdóttir H, et al. The Molecular Signatures Database (MSigDB) hallmark gene set collection. *Cell Syst*. 2015;1(6):417–425. doi:10.1016/j.cels.2015.12.004
27. Hao Y, Stuart T, Kowalski MH, et al. Dictionary learning for integrative, multimodal and scalable single-cell analysis. *Nat Biotechnol*. 2024;42(2):293–304. doi:10.1038/s41587-023-01767-y
28. Luo J, Quan J, Tsai J, et al. Nongenetic mouse models of non-insulin-dependent diabetes mellitus. *Metabolism*. 1998;47(6):663–668. doi:10.1016/S0026-0495(98)90027-0
29. Wang J, Yang N, Li W, et al. Role of hsa_circ_0000880 in the regulation of high glucose-induced apoptosis of retinal microvascular endothelial cells. *Transl Vis Sci Technol*. 2024;13(4):12. doi:10.1167/tvst.13.4.12
30. Shen W, Song Z, Zhong X, et al. Sangerbox: a comprehensive, interaction-friendly clinical bioinformatics analysis platform. *iMeta*. 2022;1(3):e36. doi:10.1002/imt2.36
31. Rübsam A, Parikh S, Fort PE. Role of inflammation in diabetic retinopathy. *Int J Mol Sci*. 2018;19(4):942. doi:10.3390/ijms19040942
32. Hu A, Schmidt MHH, Heinig N. Microglia in retinal angiogenesis and diabetic retinopathy. *Angiogenesis*. 2024;27(3):311–331. doi:10.1007/s10456-024-09911-1
33. Jiang F, Lei C, Chen Y, et al. The complement system and diabetic retinopathy. *Surv Ophthalmol*. 2024;69(4):575–584. doi:10.1016/j.survophthal.2024.02.004
34. Andrés-Blasco I, Gallego-Martínez A, Machado X, et al. Oxidative stress, inflammatory, angiogenic, and apoptotic molecules in proliferative diabetic retinopathy and diabetic macular edema patients. *Int J Mol Sci*. 2023;24(9):8227. doi:10.3390/ijms24098227
35. Huang Z, Chen LJ, Huang D, et al. Preoperative intravitreal conbercept injection reduced both angiogenic and inflammatory cytokines in patients with proliferative diabetic retinopathy. *J Diabetes Res*. 2024;2024(1):2550367. doi:10.1155/2024/2550367
36. Brandsma AM, Schwartz SL, Wester MJ, et al. Mechanisms of inside-out signaling of the high-affinity IgG receptor FcγRI. *Sci Signal*. 2018;11(540). doi:10.1126/scisignal.aaq0891

37. Nimmerjahn F, Ravetch JV. Fcgamma receptors as regulators of immune responses. *Nat Rev Immunol*. 2008;8(1):34–47. doi:10.1038/nri2206
38. Vivier D, Sharma SK, Adumeau P, et al. The impact of FcγRI binding on immuno-PET. *J Nucl Med*. 2019;60(8):1174–1182. doi:10.2967/jnumed.118.223636
39. Liu F, Shen X, Su S, et al. Fcγ receptor I-coupled signaling in peripheral nociceptors mediates joint pain in a rat model of rheumatoid arthritis. *Arthritis Rheumatol*. 2020;72(10):1668–1678. doi:10.1002/art.41386
40. Walling BL, Kim M. LFA-1 in T cell migration and differentiation. *Front Immunol*. 2018;9:952. doi:10.3389/fimmu.2018.00952
41. Balada E, Castro-Marrero J, Felip L, et al. Clinical and serological findings associated with the expression of ITGAL, PRF1, and CD70 in systemic lupus erythematosus. *Clin Exp Rheumatol*. 2014;32(1):113–116.
42. Fury MG, Lipton A, Smith KM, et al. A phase-I trial of the epidermal growth factor receptor directed bispecific antibody MDX-447 without and with recombinant human granulocyte-colony stimulating factor in patients with advanced solid tumors. *Cancer Immunol Immunother*. 2008;57(2):155–163. doi:10.1007/s00262-007-0357-5
43. Ferreira PM, Costa-Lotufo LV, Moraes MO, et al. Folk uses and pharmacological properties of Casearia sylvestris: a medicinal review. *An Acad Bras Cienc*. 2011;83(4):1373–1384. doi:10.1590/S0001-37652011005000040
44. Prinz M, Jung S, Priller J. Microglia biology: one century of evolving concepts. *Cell*. 2019;179(2):292–311. doi:10.1016/j.cell.2019.08.053
45. Nayak D, Roth TL, McGavern DB. Microglia development and function. *Annu Rev Immunol*. 2014;32(1):367–402. doi:10.1146/annurev-immunol-032713-120240
46. Tang L, Zhang C, Lu L, et al. Melatonin maintains inner blood-retinal barrier by regulating microglia via inhibition of PI3K/Akt/Stat3/NF-κB signaling pathways in experimental diabetic retinopathy. *Front Immunol*. 2022;13:831660. doi:10.3389/fimmu.2022.831660